

DISTORTION OF CRYSTAL LATTICE AND ABNORMAL INFRA-RED BEHAVIOR IN NANOCRYSTALLINE CaCO_3

YUE Lin-hai(岳林海), SHUI Miao(水淼), XU Zhu-de(徐铸德)

(*Department of Chemistry, Yuquan Campus of Zhejiang University, Hangzhou, 310027, China*)

Received Dec. 18, 1998; revision accepted July 20, 1999

Abstract: In this study, the structure of nanocrystalline CaCO_3 was analyzed using TEM, SEM, FT-IR and XRD measurements. An unusually narrow ν_3 band with remarkable blue shift about 40 cm^{-1} in the infrared spectrum was observed. XRD analysis revealed a somewhat large crystallite strain in the nano-particle CaCO_3 . The strain was possibly related to the weakened lattice vibration. This suggests a preliminary explanation for the abnormal IR assimilation characteristics of nanocrystalline CaCO_3 aforementioned.

Key words: nanocrystalline calcite, distortion of crystal lattice, infrared behavior

Document code: A **CLC number:** TQ115

INTRODUCTION

The nano-particle CaCO_3 has attracted more and more research interest because of its broad applications in industrial fields. Many researchers tried to explain the abnormal characteristics of nano-material from the viewpoint of the crystal structure and crystal interfacial volume fraction. It was proposed that most materials' crystal grains contract with the diminution of the particle size, but some materials behave otherwise, nanocrystalline MgO for example. This contraction (or expansion) of crystal grains results in the distortion of the crystal lattice (Ye et al., 1998), which is normally called size effect, and further influences the physicochemical properties such as infra-red assimilation behavior. For most of the nano-materials, blue shift and broadening of the absorption peaks will occur with the diminution of particle size (Ball et al., 1992; Zhang et al., 1994). However, some nano-materials show both blue shift and red shift of the infra-red absorption peaks under the influence of the crystal expansion and hydrogen bonds (Ye et al., 1998).

As is well known, the free carbonate ion belongs to the point group D_{3h} and therefore has four normal vibrations: one of species A_1' , one of species A_2' , two of species E' . A_1' is Raman active, A_2' is IR active and the other vibration modes are both Raman and IR active, so three absorption peaks should appear in the infrared

spectrum. Relatively large strain in the crystal lattice of nano-particle CaCO_3 was revealed by X-ray diffraction measurements and Voigt function analysis in this study. A remarkable blue shift and an unusually narrow ν_3 band in the mid-infrared spectrum were observed, which finding has never been reported in the literature to the author's knowledge. We suggest that the size effect and crystal distortion in the lattice of nano-particle CaCO_3 weaken the crystal field effect and lattice vibrations, and finally result in the abnormal IR behavior.

THEORIES

Voigt function analysis, in conjunction with breadth parameters including $2w$ (FWHM) and β (integral breadth) of diffraction line profile, forms the basis of a powerful method for routine studies of crystallite size and strain. A limitation in the use of the FWHM or integral breadth method is the need to ascribe an analytical function to the diffraction line profiles. Different profile functions were reviewed by Yong and Wiles (Yong et al., 1982). Several authors conducted comparative studies on subsets of the six analytical functions, Gaussian (G), Lorentzian (L), modified Lorentzian (ML), intermediate Lorentzian (IL), pseudo-voigt (P-V), and pearson VII (P-VII). Most of the results showed that the voigt function can simulate the experimental curve best (Yong et al., 1982).

The voigt function $I(x)$ can be regarded as the convolution of the Cauchy and Gaussian function(Langford, 1978),

$$I(x) = \int_{-\infty}^{\infty} I_C(u) I_G(x - u) du \quad (1)$$

where subscript C and G represent Cauchy and Gaussian function, respectively.

Fourier transformation of $I(x)$ yields

$$I(x) = Re \left\{ \beta_C I_C(0) I_G(0) \omega \left[\frac{\pi^{1/2} x}{\beta_C} + ik \right] \right\} \quad (2)$$

in which $k = \beta_C / \pi^{1/2} \beta_G$, ω is the complex error function.

The integral breadth, β , is (de Keijser et al., 1982)

$$\beta = \frac{\beta_C e^{-k^2}}{1 - \text{erf}(k)} \quad (3)$$

The full width at half the maximum intensity of the Voigt function, $2w$, can be obtained from

$$Re \left\{ \omega \left[\frac{\pi^{1/2} x}{\beta_C} + ik \right] \right\} = \frac{1}{2} \omega[ik] = \frac{\beta_C}{2\beta} \quad (4)$$

where β_G and β_C are the constituent Gaussian and Cauchy components of the diffraction line profile.

The relationship between the form factor of the Viogt function $2w/\beta$ and the constituent Gaussian and Cauchy components β_G and β_C determined by Eq. 1, Eq.2 and Eq.3 respectively can be illustrated by a graphical curve (Fig. 1).

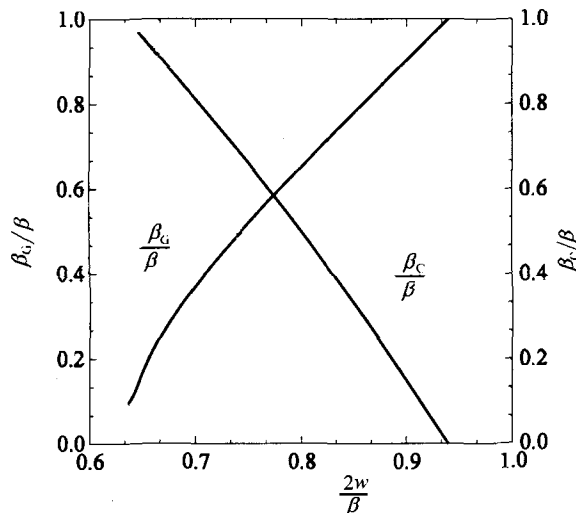


Fig.1 The form factor $2w/\beta$ of the measured line profile vs. constituent Cauchy component β_C and Gaussian component β_G

We assume that the measured line profile $h(x)$, instrumental broadening profile $g(x)$ and the structurally broadening profile $f(x)$ are all Voigt functions, and have the relation (de Keijser, et al., 1982).

$$h_c = g_c \times f_c, \quad h_G = g_G \times f_G \quad (5)$$

From Eq. 5 it follows that the integral breadths of f_c and f_G are given by

$$\beta_c^f = \beta_c^h - \beta_c^g, \quad (\beta_G^f)^2 = (\beta_G^h)^2 - (\beta_G^g)^2 \quad (6)$$

In the single-line analysis it is assumed that the Cauchy component of the measured line profile is solely due to crystallite size and that the Gaussian contribution arises from crystallite strain. There are theoretical justifications for this assumption and experimental evidence has also been reported. So, in a single-line analysis, the apparent crystallite size or domain size D is given by

$$D = \lambda / \beta_c^f \cos(\theta) \quad (7)$$

and the crystallite strain e by

$$e = \beta_c^f / 4 \tan(\theta) \quad (8)$$

where β_c^f and β_G^f are measured on a 2θ scale. λ and θ are wave length and angular position of the $K_{\alpha 1}$ component when K_{α} radiation is used.

Therefore, when the integral breadth and FWHM of the measured profile and instrumental broadening profile are obtained from the experimental data, β_c^f and β_G^f can be deduced according to Eq.6 and Fig. 1. Afterwards, Eq.7 and Eq. 8 can be used to calculate the crystallite size and crystallite strain.

EXPERIMENTAL SECTION

Purified CO₂ gas (20 ~ 40% concentration, diluted with N₂) was bubbled through 5 ~ 10% Ca(OH)₂ until the pH was at 7 ~ 8. The precipitate was filtered, dried at 110 °C to steady weight and then sifted through 320 mesh. Under altered reaction conditions three nano-particle CaCO₃ samples with different particle size and crystal form were obtained, and named as 980227c, 980602 and 980622, respectively (Cai et al., 1995).

X-ray powder diffraction patterns were obtained at room temperature by a Philips diffrac-

tometer model X Pert MPD using Cu K_{α} radiation at scanning step 0.02° and scanning rate $1^{\circ}/\text{min}$. PC-APD 4.0 software was used to separate $K_{\alpha 2}$ from $K_{\alpha 1}$ and Philips Profile Fit to obtain $2w$ and β .

The IR spectra were recorded at room temperature in the region of $400 \sim 3600\text{cm}^{-1}$ with a Nicolet FT-IR model 5DX spectrometer using KBr pellets.

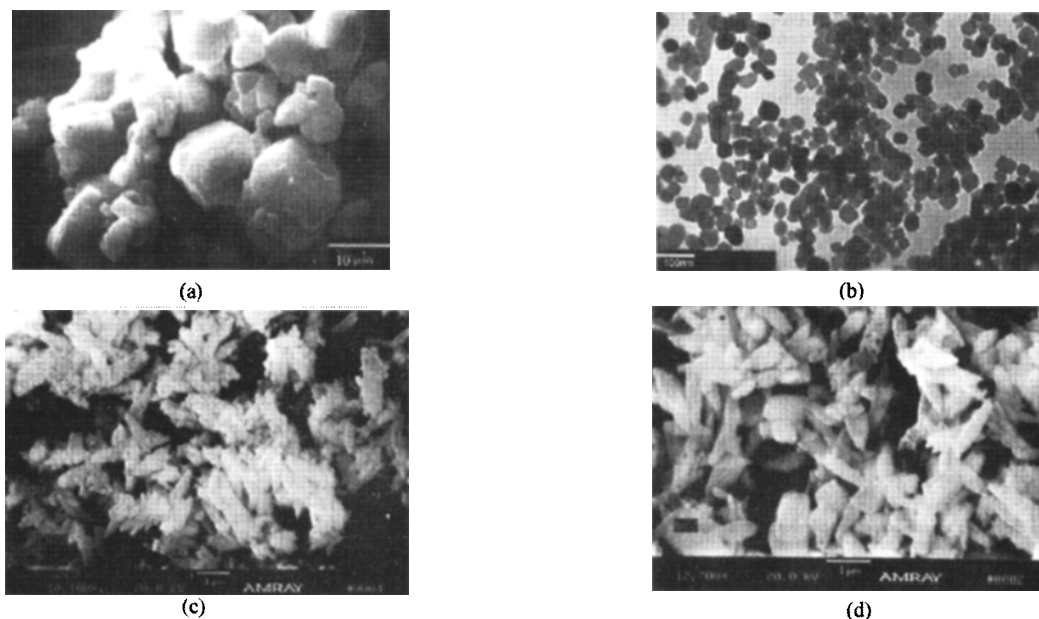


Fig.2 SEM or TEM images of Samples

(a) reference samples; (b) sample 980227c; (c) sample 980602; (d) sample 980622.

Calcite (99.99%, $5 \sim 20\mu\text{m}$ particle size estimated by SEM, see Fig. 2a) was used as reference sample without structural broadening. The XRD pattern of the reference calcite with Bragg angle of 20° to 70° was obtained under the same condition. Fig. 3 shows the integral breadth β and

FWHM $2w$ of the instrumental broadening profile varying with the variation of Bragg angle 2θ .

RESULTS AND DISCUSSION

1. Crystal structure of the nanocrystalline CaCO_3

The TEM or SEM images of the three nanoparticle CaCO_3 samples are shown as Fig. 2b, Fig. 2c and Fig. 2d. The above TEM images show that sample 980227c had a cubic structure crystal lattice with particle size of 40 to 80 nm. Sample 980622 had a shuttle-form structure, about $1.5 \sim 2\mu\text{m}$ long and $300 \sim 600\text{nm}$ wide. The crystal lattices of both two samples seem integrated. There were also a few $100 \sim 400\text{nm}$ cubic grains mixed with the shuttle-form grains. Most of the crystal grains in sample 980602 had loose shuttle-form structure, about $1 \sim 1.5\mu\text{m}$ long and $200 \sim 600\text{nm}$ wide. The sample also had a considerable number of $100 \sim 500\text{nm}$ cubic grains. The sample with the structure shown in Fig. 2c seems to be in

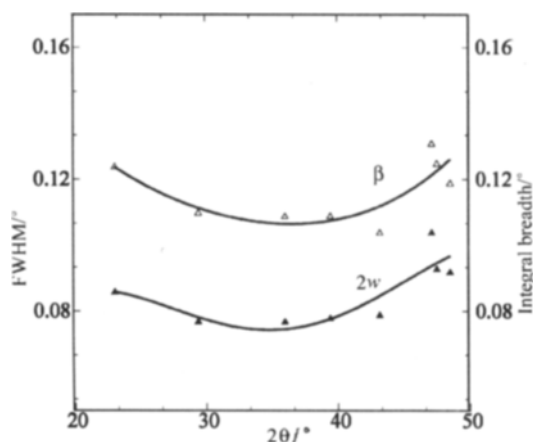


Fig.3 The FWHM $2w$ and integral breadth β of instrumental broadening vs. 2θ

the process of the conglomeration of base structure as Fig. 2b shows.

Fig. 4 of the X-ray diffraction pattern of sam-

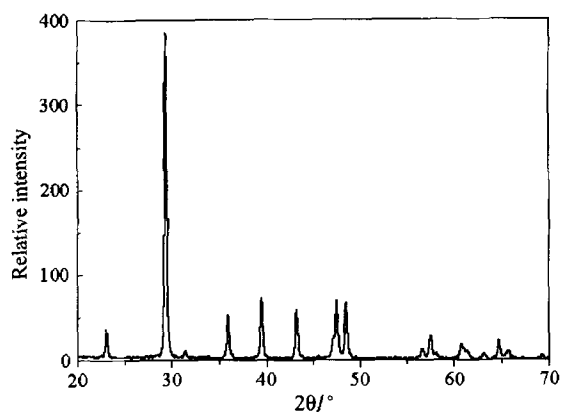


Fig. 4 The X-ray diffraction spectrum of sample 980227c.

ple 980227c shows that the intensity and the distance between crystal planes of diffraction peaks for the three nano-particle CaCO₃ samples are in good agreement with the standard spectrum of the crystalline polymorphs calcite of calcium carbonate (ICDD, 1993). The comparison assures us that the three samples were all calcite. Fig. 5 shows the diffraction line profile of (110) plane for the

three nano-particle CaCO₃ samples and the reference sample. Obviously, the diffraction line profiles of the three samples are broader than that of the reference CaCO₃. The FWHM, integral breadth, crystallite size and strain of the three nano-particle CaCO₃ samples for the (110), (113) and (202) planes diffraction line profile are listed in Table 1.

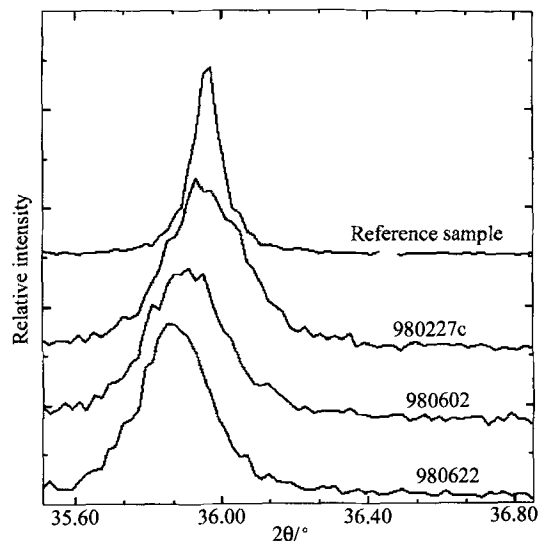


Fig. 5 X-ray diffraction intensity curve of (110) plane for reference calcite, sample 980227c, 980602 and 980622.

Table 1 The experimental data of (110), (113), (202) plane X-ray diffraction for three samples and the results of Voigt function analysis

Parameters		980227c	980602	980622
(110)	2θ(°)	35.914	35.869	35.841
	2ω(°)	0.212	0.216	0.182
	β(°)	0.289	0.292	0.243
	e × 10 ³	1.7	1.8	1.6
	D(nm)	77.8	79.9	123.5
(113)	2θ(°)	39.364	39.320	39.279
	2ω(°)	0.217	0.195	0.200
	β°	0.297	0.278	0.278
	e × 10 ³	1.6	1.2	1.4
	D(nm)	71.8	55.0	74.2
(202)	2θ(°)	43.097	43.047	43.018
	2ω(°)	0.210	0.228	0.193
	β(°)	0.283	0.319	0.268
	e × 10 ³	1.4	1.3	1.1
	D(nm)	73.8	52.8	69.7

The strain in the nanocrystalline calcite was about 1.2 ~ 1.8‰ and was relatively large. The lattice strain distribution is uniform in the different diffraction directions or between three nanoparticle calcite samples. From the TEM or SEM images, we can see that the crystal grains of sample 980227c were cubic and that the crystallite sizes in the different diffraction directions listed in Table 1 were close to each other, averaging 75nm. Sample 980622 was composed of shuttle-form grains whose crystallite sizes in the different diffraction directions varied, and were not in accord with the particle size obtained from TEM or SEM images but were close to those of sample 980227c. Sample 980602 had a loose shuttle-form structure. The variation of crystallite size in the different diffraction directions was in-between that of the other two samples. We suggest that crystal grains constituting sample 980622 were formed by crystal growth of the base structure shown in Fig. 2b on the different crystal planes. The coexistent appearance of loose shuttle-form grains and cubic grains shown in Fig. 2c to a certain extent shows the process of conglomeration. This loose conglomeration explains the crystallite distribution listed in Table 1 and the diversity of calcite crystal forms.

2. The infra-red behavior of nanocrystalline CaCO₃

The infrared spectra of three nano-particle CaCO₃ samples and reference CaCO₃ are shown in Fig. 6. The main peak positions on the infrared spectrum of reference CaCO₃ are $\nu_3 = 1425\text{cm}^{-1}$, $\nu_2 = 874\text{cm}^{-1}$ and $\nu_4 = 712\text{cm}^{-1}$. The ν_3 band is strong and broad while ν_2 and ν_4 bands are weak and narrow. According to the calcite standard infrared spectrum (SRLI, 1974) and reports from Andersen et al. (1991), the crystal structure of the reference sample is calcite. The main peak positions of the three nano-particle CaCO₃ samples are estimated at 1465cm^{-1} , 875cm^{-1} and 713cm^{-1} , respectively. The ν_3 band has a 40cm^{-1} blue shift compared with the reference and contrary to previous reports of broadened assimilation bands in nanomaterials, is unusually narrow. The fact that the ν_2 and ν_4 bands are not split denotes that the crystal structures of the three nano-particle CaCO₃ samples were calcite. Andersen et al. (1991) suggested that the strong and broad ν_3

assimilation band originated from several overlapping bands resulted from the combination of lattice vibration of A_{2u} (354cm^{-1}), E_u (311cm^{-1} , 227cm^{-1}) and ν_2 , ν_4 bands. Rao (1963) suggested that the crystal field effect often caused the broadened absorption bands. Therefore, we suggest that many defects or relatively large strains in the crystal lattice of nanoparticle calcite weaken the crystal field effect and, weaken the lattice vibrations of A_{2u} and E_u in the far infrared region as well. Consequently, the overlapping peaks around the ν_3 band disappear and the ν_3 band seems narrow.

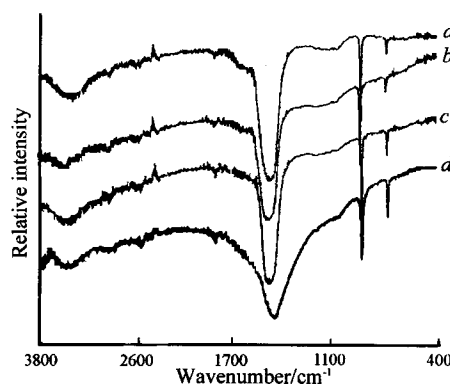


Fig. 6 The infra-red spectra for sample a. 980227c; b. 980602; c. 980622; d. reference calcite.

CONCLUSIONS

1. The ν_3 absorption band of nanocrystalline calcite in the infrared spectrum has an obviously 40cm^{-1} blue shift and is unusually narrow. The many defects or relatively large strain in the crystal lattice revealed by XRD measurements weaken the crystal field effect and weaken the lattice vibrations A_{2u} and E_u in the far infrared region as well. Therefore, the combination of lattice vibration modes and the ν_2 , ν_4 bands around the ν_3 band disappear and the ν_3 band seems narrow.
2. An analysis of the three nano-particle calcite samples shows that the conglomeration of the base crystal grains causes the diversity of crystal form. Therefore, products having different crystal forms, usually having different applications in industrial fields, can be obtained by controlling reaction conditions (Yue, et al., 1994).

ACKNOWLEDGMENTS

The authors are very thankful for the valuable help of Professor Liu Qing in IR measurements and Professor Ding Chenghao, Zheng Yifan in XRD measurements and analysis.

References

- Andersen, A., Ljerka B., 1991. Infrared spectra of amorphous and crystalline calcium carbonate. *Acta Chemica Scientia*. **45**:1018 - 1024.
- Ball, P., Garwin L., 1992. Science at the atomic scale. *Nature*. **355**: 761 - 766.
- Cai Juxiang, Yue Linhai, 1995. Study on the synthetic terms of ultrafine CaCO₃. *Inorganic Salt Industry*. **5**(7): (in Chinese, with English abstract)
- de Keijser TH. H., Langford J. I., Mittemeijer E. J. et al., 1982. Use of the voigt function in a single-line method for the analysis of X-ray diffraction line broadening. *J. Appl. Cryst.*, **15**: 308 - 314.
- ICDD, 1993. Mineral Powder Diffraction File Data Book, No.5 - 586.
- Langford, J. I., 1978. A rapid method for analyzing the breadths of diffraction and spectral lines using the voigt function. *J. Appl. Cryst.*, **11**: 10 - 14.
- Rao C. N. R., 1963. Chemical applications of infrared spectroscopy. Academic Press, London, p.23.
- Sadtler Research Laboratory Inc., 1974. Sadtler commercial spectra IR grating inorganics, Vo.1, No.y41K.
- Ye Xisheng, Sha Jian, 1998. Distortion of crystal lattice and abnormal infrared behavior in nanocrystalline MgO. *Function Materials*. **29**:287 - 289. (in Chinese with English abstract)
- Zhang Lide, Mou Jimei, 1994. Science of nanomaterial. Liaoning Sci. Pub., Shenyang p.30(in Chinese).
- Yong, R. A., Wiles D. B., 1982. Profile shape functions in rietveld refinements. *J. Appl. Cryst.*, **15**: 430 - 438.
- Yue Linhai, Cai Juxiang, Jing Nanping, 1994. The New Inorganic Reinforced Filler —Ultrafine CaCO₃, *Zhejiang Chem. Eng.*, **25**: 7 (in Chinese with English abstract).